RESEARCH ARTICLE OPEN ACCESS

Performance assessment of Boost, Cuk and Zeta converter with Neural Network MPPT in PV Systems for Varying Weather Patterns

R Divyasharon*, R Narmatha Banu**
*(Department of Electrical and Electronics Engineering, Velammal College of Engineering and Technology, Madurai-625009, India.)
** (Department of Electrical and Electronics Engineering, Velammal College of Engineering and Technology, Madurai-625009, India.)

ABSTRACT
Renewable energy is a possible choice that will optimistically guide us away from fossil fuels. Among them, Solar Photovoltaic (SPV) energy is an inevitable form of renewable energy. A DC-DC converter functions as an interface connecting SPV panels and the load for transferring maximum power. Here, the DC-DC power converter is tuned by a Maximum Power Point Tracking (MPPT) controller to exploit the solar array at a maximal power point. Frequently employed MPPT approaches namely Incremental Conductance (IC) and Perturb and Observe (P-O) provides sustainable performance under uniform atmospheric condition but the tracking gets complex under fluctuating atmospheric conditions. Here, the MPPT controller is built for the DC-DC converter utilizing Artificial Neural Network (ANN) since the method of approximation is quick, accurate, and robust. The systems were developed with Zeta and Cuk converters to provide efficient performance, and the execution is calculated with the Boost-Converter. The performance assessment of MPPT based on P-O and ANN with all converters was studied using the software MATLAB/Simulink for uniform and different atmospheric conditions. The simulation outcomes depicted that the implementation of ANN based MPPT algorithm with zeta converter exhibited a more efficient output power range than Cuk and Boost converter in all fluctuating climatic conditions with controller efficiency rate of 99.50% and converter's efficiency rate 99.8% in gaining out maximum power tracking process.

Keywords - Artificial neural networks, DC-DC power converters, Maximum power point tracking, Photovoltaic systems, and Renewable energy sources

Date of Submission: 04-04-2022 Date of Acceptance: 19-04-2022

I. INTRODUCTION

Solar Photovoltaic (SPV) is the most significant feasible and plentiful energy source of all renewable energy sources. It is an eco-friendly form of energy that does not generate any hazardous gases. Despite several advantages, the conversion efficiency of the SPV system is reduced substantially. The SPV system's conversion capability largely depends on three variables: the capacity of the solar cell, the power converter, and the potentiality of the MPPT technique. The enhancement of the MPPT techniques is the preferred choice to increase the effectiveness and simplicity of operation of photovoltaic systems. The maximum power point is nevertheless regularly changed by solar radiation and temperature; under almost all situations it is crucial and hard to monitor the Maximum Power Point (MPP). Several MPPT approaches are presented in the studies [1-4]. Traditional MPPT methods and advanced MPPT methods are the primary groups. They have got two major groupings. The first includes Hill climbing (H-C), Perturbation and Observation (P-O), Incremental conductance (I-C). The latter usually comprises Artificial Neural Networks, Evolutionary Algorithms, and Fuzzy Logical Controllers, widely used recently because they are able to deal with the linear, non-linear, complicate and insufficient patterns of data in terms of their resilience, logical reasoning and interpretation potentials and their capacity in learning. However, in terms of efficiency and response time, the ANN controller demonstrated good performance in rapidly changing situations [5, 6].

The design of the converter renders a crucial part in every method of tracking. The MPPT tracker-controlled converter is used to match the load and maximize the power of the SPV panel [7]. A DC-DC converter is attached in the middle of the load and the SPV panel with an MPPT controller to detect that the PV is operated near MPP [8]. DC-DC converters are frequently grouped into two classes: Isolated and Non-isolated DC-DC converters. Non-isolated converters are easy to design and cost-effective in contrast with isolated converters. Many non-isolated converters are suggested in the literature [9]. This work describes the design and analysis of Boost, Cuk, and Zeta converters under varying atmospheric conditions.

A Boost converter furnishes higher output voltage in comparison with source voltage. It is typically employed to regulate the input supply ad to significantly enhance the line power factor.

A Cuk converter may be employed to interface nearly matched load or battery to module voltages as it furnishes output voltage with reversed polarity and magnitude less, equivalent or greater than that of the input voltage. A Cuk converter has distinct benefits namely capacitive energy transfer, broad transformation ratio, continuous input and output current, and complete usage of transformer. [10].

The Zeta converter is a choice to regulate the unregulated supply of input power. This Zeta converter is utilized to offer positive output obtained from input voltage, wherein it is also used to maximize or minimize the voltage level. Some of the application usages of Zeta converters are in short-circuit protection and in Power-factor correction application.

In this paper, traditional P&O and proposed ANN-based MPPT are realized by Boost, Cuk and Zeta converter for changing irradiance and temperature conditions and their capabilities are evaluated for constant and fluctuating atmospheric circumstances.

II. MATERIALS AND METHODS

2.1 System Design

The SPV system incorporates a SPV panel, DC-DC power converter, MPPT tracker and a load.

Fig.1 displays the SPV system with the proposed control algorithm. DC-DC converters employed here are Boost, Cuk and Zeta converters. MPPT controllers used in this work are P&O and ANN based MPPT controllers.

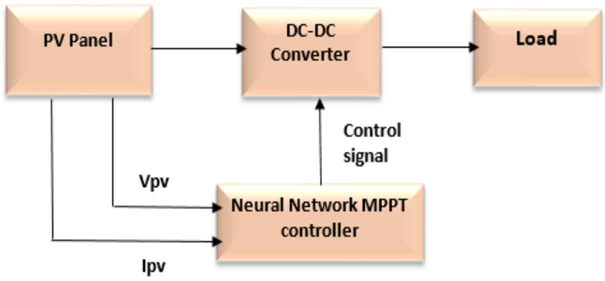

Figure 1: SPV system representation with the proposed control algorithm

2.2 Solar PV Panel Model

An SPV cell is an electrical device that creates electricity from light energy. Several SPV cells are linked in parallel or serially to create an SPV module and an array is created by numerous SPV modules. Typically, an SPV structure displays nonlinear I-V and P-V attributes that alters by irradiance and temperature [15]. Fig.2 depicts the electrical representation of the SPV cell

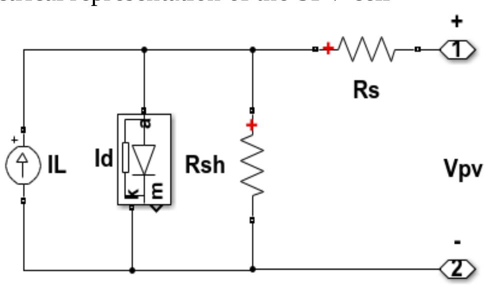

Figure 2: Solar PV cell electrical diagram

The current output of the SPV module is specified by

$$I_{pv} = I_L - I_o\left[exp\left(\frac{q(V_{pv}+I_{pv}R_s)}{kTAN_s}\right) - 1\right] - \frac{(V_{pv}+I_{pv}R_s)}{R_{sh}} \quad (1)$$

where I_{pv} -SPV array's current output, V_{pv} -SPV array's voltage output, I_L - current generated by light, R_{sh} and R_s a- shunt and series resistance correspondingly, A-ideality factor of diode,, q-electronic charge ($1.602\times10^{-19}C$), k-Boltzmann constant (1.38×10^{-23}J/K), and T - temperature of the cell. The reverse saturation current I_o is

$$I_o = I_{oref}\left[\frac{T}{T_r}\right]^3 \exp\left[\frac{qE_g}{kqA}\left(\frac{1}{T_r} - \frac{1}{T}\right)\right] \quad (2)$$

Where Tr - reference cell temperature and E_g - semiconductor's bandgap energy.
The photocurrent Iph relies on solar PV irradiance and temperature of the cell as follows:

$$I_{ph} = [I_{sc} + k_c (T - T_r)] \frac{G}{1000} \quad (3)$$

Where I_{sc}-short circuit current, G denotes solar irradiance, k_c denotes short circuit current's temperature coefficient.
The solar PV array power can be stated as

$$P_{pv} = I_{pv} V_{pv} \quad (4)$$

Table 1: PV panel Specifications

PV PANEL CHARACTERISTICS	VALUE
Maximum power (P_{max})	100 W
Current-Short circuit (I_{sc})	6.30 A
Current-Maximum power (I_{mpp})	5.70 A
Voltage-Open circuit (V_{oc})	21.40 V
Voltage-Maximum power (V_{mpp})	17.70 V
Resistance-Shunt (R_{sh})	56.570 Ω
Resistance-Series (R_s)	0.170 Ω
Ideality factor of diode	0.96540

Table 1 presents the solar panel characteristics employed in this paper.1000W SPV array is formed by connecting two 100W panels serially and five of those panels are linked in parallel.

2.3 Converter Modeling

The Maximum Power Point of the SPV model differs with fluctuating atmospheric situations and the MPPT regulator must modulate the duty cycle of the converter for tracing the new MPP. Therefore, the converter used should be equipped to match the MPP with altering environmental situations. In addition to the limit of the converter design parameters, due to the environmental change, the duty cycle will vary. So, these parameters should be determined suitably to obtain good performance at changing atmospheric circumstances. This article compares Boost converter, Cuk and Zeta converter for constant and fluctuating atmospheric circumstances.

2.3.1 Boost Converter

A Boost converter is otherwise known as a step-up chopper as the output voltage is of higher magnitude in comparison with the source voltage. It belongs to a second-order converter and it functions by a single switch. Fig.3 displays the electrical representation of the Boost converter. The diode becomes reverse biased thereby inducing a raise in current across the inductor while the switch is in ON condition. The diode is forward biased and hence the energy in the inductor is transferred from the storage element to the load when the switch is in OFF condition [11].

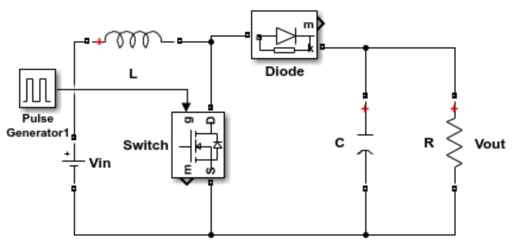

Figure 3: Electrical representation of a Boost converter

Design equations of Boost converter:

$$\frac{V_{out}}{V_{in}} = \frac{1}{(1-D)} \quad (5)$$

$$L = \frac{V_{in}(V_{out} - V_{in})}{\Delta I_L f_s V_{out}} \quad (6)$$

$$C = \frac{I_{out} D}{f_s \Delta V_{out}} \quad (7)$$

Wherein D-duty cycle of the converter and f_s-switching frequency. Table 2 denote the specifications of Boost converter.

2.3.2 Cuk Converter

The output voltage of the converter is higher or lesser in contrast with the supply voltage with opposite polarity. Boost converter is the source side and the Buck converter is the output side. A

Cuk converter possesses numerous benefits namely capacitive energy transfer, continuous input and output current, broad transformation ratio, and complete usage of transformer. Fig.4 depicts the electrical representation of Cuk converter.

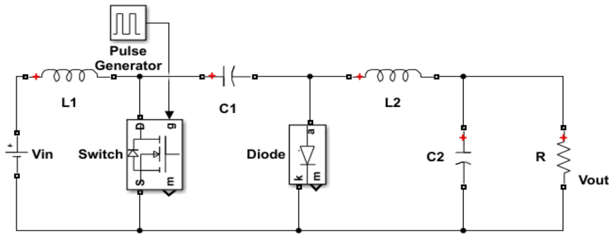

Figure 4: Electrical representation of a Cuk converter

The current i_{L1} creates the magnetic field of the inductor and the energy is transferred across the inductor to the load when the switch is ON. The inductor L_1 attempts to sustain the current flow by reversing the polarity and thus transferring energy to the load through Capacitor C_1 while the switch is OFF [11].
Design equations of Cuk converter:

$$\frac{V_{out}}{V_{in}} = -\frac{D}{(1-D)} \tag{8}$$

$$L_1 = \frac{(1-D)^2 R}{2Df_s} \tag{9}$$

$$L_2 = \frac{(1-D)R}{2f_s} \tag{10}$$

$$C_1 = \frac{DV_o}{V_r R f_s} \tag{11}$$

$$C_2 = \frac{(1-D)}{8V_r L_2 f_s^2} \tag{12}$$

Whereas D-duty cycle of the Cuk converter, f_s-switching frequency and V_r-ripple voltage. Table 2 presents the specifications of the Cuk converter.

2.3.3 Zeta Converter

In this proposed framework, the Zeta converter has been selected due to its benefits exhibiting adaptability, lesser settling-time that could be interfaced with a higher range of frequency transformers. The Zeta converter circuit diagram has been described in fig.5. Zeta converter can convert the input voltage into non-inverted output voltage. This output voltage has a higher value or possesses a lower value than the value of input voltage. This converter is suitable for operating the discontinuous operation modes and also continuous operation modes. The ON state of Zeta converter is attained in the following condition such that the power electronic switch is ON and Diode-D is in OFF. The power or energy across the inductor L_1 and L_2 were retrieved from V_s- voltage source. Meanwhile, the current in L_1 and L_2 are increasing linearly. This type of mode operation is referred to as charging mode. While the switch is in OFF state and the diode possess ON state, the energy which is saved in inductors L_1 and L_2 does discharges and the transfers into load. The power within the inductors linearly decreases in this model. Hence this operation mode is referred as the discharging operation mode of Zeta converter.

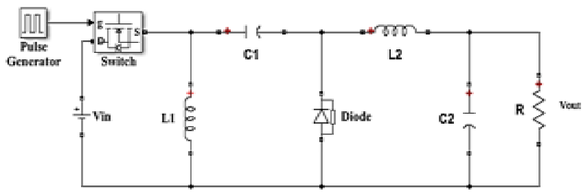

Figure 5: Electrical representation of a Zeta converter

The consecutive equations are employed to design the Zeta converter:

$$D = \frac{V_{out}}{V_{in} + V_{out}} \tag{13}$$

$$\frac{V_{out}}{V_{in}} = \frac{D}{(1-D)} \tag{14}$$

$$L_1 = \frac{V_{in} D}{2\Delta I_L f_s} \tag{15}$$

$$L_2 = \frac{V_{in} D}{2\Delta I_{L2} f_s} \tag{16}$$

$$C_1 = \frac{DI_o}{\Delta V_c f_s} \tag{17}$$

$$C_2 = \frac{\Delta I_L}{8\Delta V_c f_s} \tag{18}$$

Table 2. Specifications of converters

COMPONENT	VALUE		
	Boost	***Cuk***	***Zeta***
L_1	55 µH	100 µH	100 µH
L_2	-	100 µH	100 µH
C_1	230 µF	200 µF	50 µF
C_2	-	20 µF	1 mF
R	2.5 Ω	2.5 Ω	2.5 Ω
f_s	50 KHz	50 KHz	50 KHz

2.4 Maximum Power Point Tracking

MPPT technique is applied for computation of duty cycle of the converter. The fundamental aim of the MPPT technique is to get peak output from the PV panel despite changes in the environment. Many control approaches are available for maximum power tracking [12]. Much prevalent control technique are Incremental Conductance and Perturbation and Observation methods. They generally perform well during constant irradiance and temperature conditions. However, these algorithms struggle to track maximum power under various environmental conditions. This project implements P&O and ANN based MPPT techniques for tracking maximum power and evaluating its performance in constant and fluctuating climatic situations.

2.4.1 Perturb and Observe (P-O) based MPPT.

The Perturb and Observe (P-O) algorithm is frequently utilized in solar photovoltaic systems because of its simplicity and its easy deployment [3], [4].

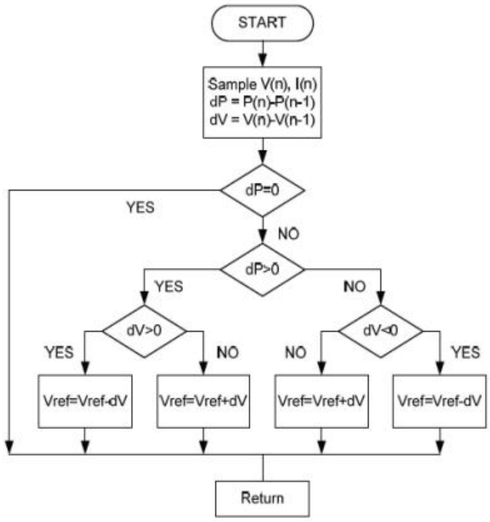

Figure 8: Flow diagram of P-O algorithm

The principle of this algorithm is to introduce a perturbation which changes the PV power. When ΔP/ΔV >0, the voltage is improved by adding ΔD. When ΔP/ΔV <0, the voltage is reduced by subtracting ΔD. This process is continued till the MPP is acquired [3]. The flow diagram of P-O algorithm is explained in fig .8.

2.4.2. Artificial Neural Network based MPPT.

Artificial Neural Networks can be seen as equivalent and dispersed information processing structures that comprise several processing units named neurons. The net consists of a considerable number of processing elements named neurons. They are interconnected by directed links with an associated weight.

The multilayer feedforward architecture that employs a backpropagation approach is employed to correct the biases and the weights. ANN includes 3 layers, the input, the hidden and the output layer as presented in fig.9. The input layer comprises 2 neurons (Temperature (T) and Irradiance (G)), the hidden layer comprises 5 neurons, and the output layer comprises 2 neurons (Maximum current (Impp) and maximum voltage (Vmpp). Levenberg Marquardt (LM) algorithm, a rapid approach is employed for training the network. Fig. 9 depicts the proposed topology of the artificial neural network.

An activation function employed by the hidden layer is 'tansig'. An activation function employed by the output layer is 'purelin'. Irradiation is varied in accordance of 100W/m2 and temperature in accordance of 5 degrees are defined as inputs and corresponding I-V and P-V graphs are plotted and the voltage and current at the peak power are estimated.

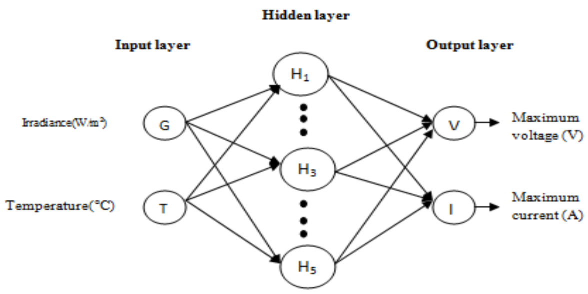

Figure 9: Topology of Neural Network

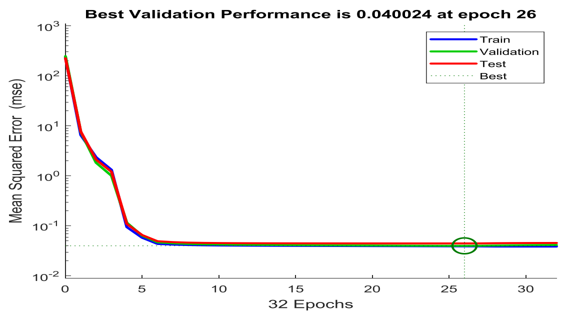

Figure 10: Performance of Neural Network

500 samples as mentioned above are acquired. In the samples, 70% is employed to train the network and 30% is employed to test the network. Once the training is completed, the network is introduced to the system to ascertain maximum voltage proportional to irradiance and temperature. The deviation in Vmpp and Vpv is fed as the duty cycle of the converter [13]. Fig.10 depicts the execution of the neural network.

III. RESULTS AND DISCUSSIONS

The system is designed in MATLAB/Simulink for changing atmospheric circumstances. Fig.11 and fig.12 depict the I-V and P-V graphs of the array at changing irradiance and static temperature correspondingly. Fig.13 and fig.15 depict the I-V and P-V curves of the array at changing temperature and static irradiance correspondingly.

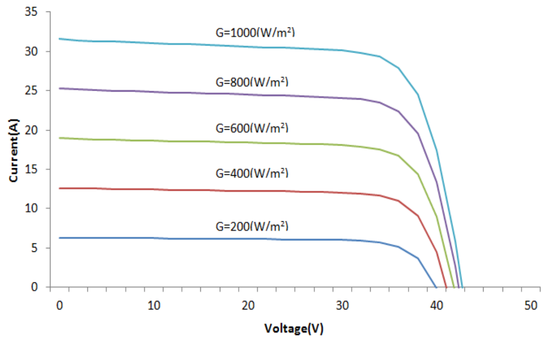

Figure 11: I-V graph of SPV array under different irradiation conditions

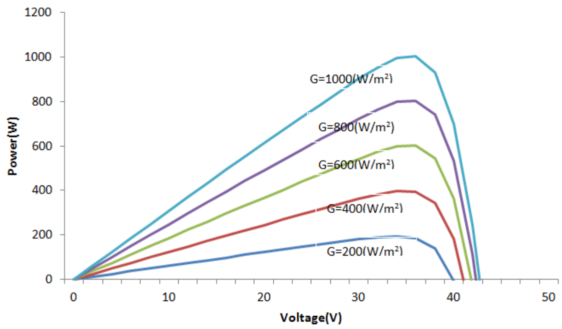

Figure 12: P-V graph of SPV array under different irradiation conditions

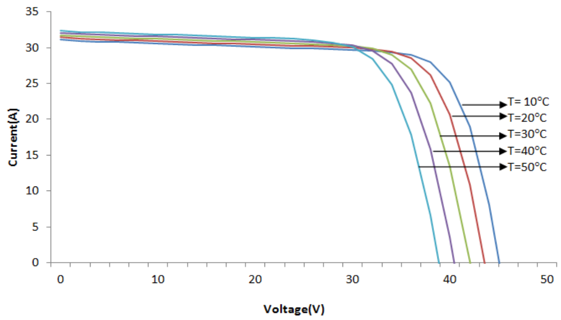

Figure 13: I-V graph of SPV array under different temperature conditions

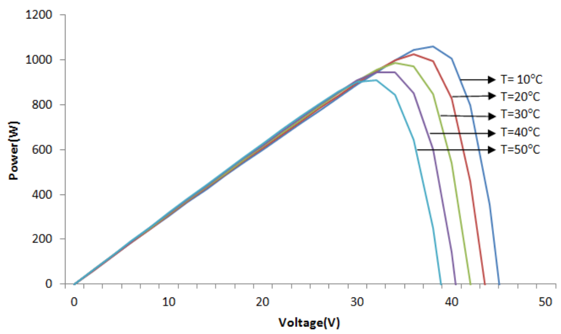

Figure 14: P-V graph of SPV array under different temperature conditions

The performance of P-O and ANN based MPPT for all three converters were examined under uniform and non-uniform atmospheric circumstances. The system is evaluated with three distinct cases. Firstly, at uniform irradiance and temperature circumstances. Secondly at the change in irradiance with fast ramp sequence and third at the change in irradiation with slow ramp sequence.

3.1 Case 1: At uniform Temperature (T) and Irradiance (G).

The output power of P-O and ANN based MPPT for the three converter under constant irradiation (G=1000 W/m^2) and temperature (T=25°c) is shown in figs.15, 16 and 17 respectively.

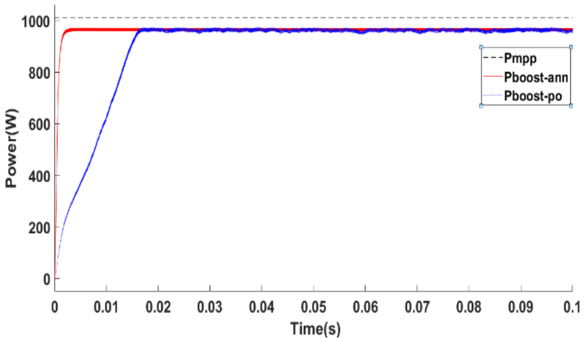

Figure 15: Boost converter output for uniform condition

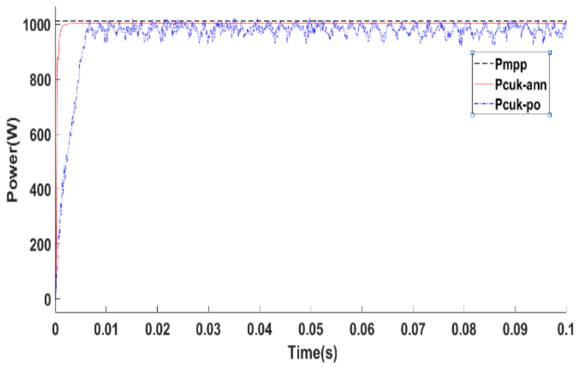

Figure 16: Cuk converter output for uniform condition

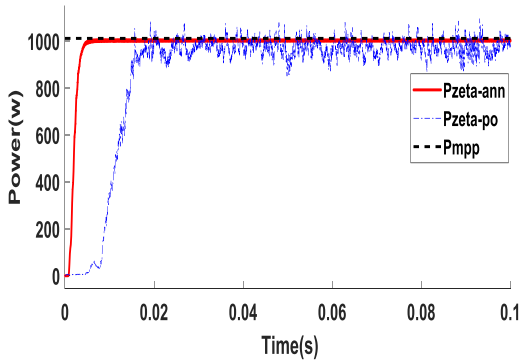

Figure 17: Zeta Converter output for uniform condition

Pmpp denotes the maximum power of the SPV array. Pboost-ann and Pboost-po represent the output power of ANN and P-O MPPT using Boost converter respectively. Pcuk-ann and Pcuk-po represent the output power of ANN and P-O MPPT using Cuk converter respectively. Pzeta-ann and Pzeta-po define the output power of ANN and P-O MPPT using Zeta converter respectively.

It is obvious from the results that the ANN based MPPT furnishes better performance for all these three converters. Between the converters, Zeta converter furnishes increased efficiency than the Boost and Cuk converters.

3.2 Case 2: At the change in irradiance with fast ramp sequence.

The input as depicted in fig.18 is introduced to the system and its equivalent power output observed employing P-O and ANN based MPPT for three converters are shown in figs.19, 20 and 21 respectively.

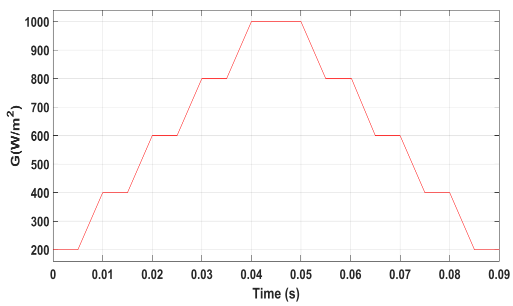

Figure 18: Irradiation change (Fast ramp sequence)

ISSN: 2248-9622, Vol. 12, Issue 4, (Series-I) April 2022, pp. 09-20

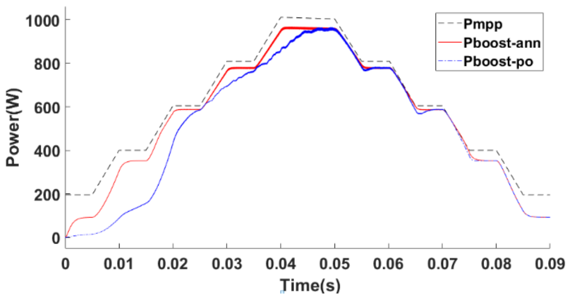

Figure 19: Boost converter output with fast ramp sequence

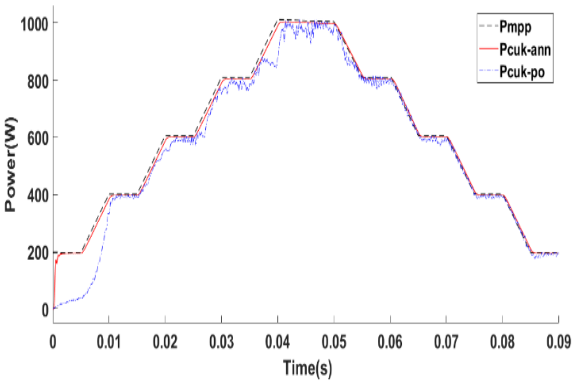

Figure 20: Cuk converter output with fast ramp sequence

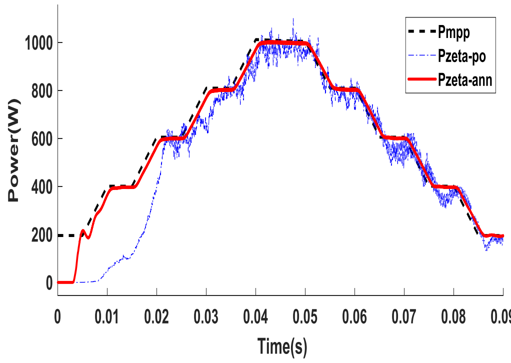

Figure 21: Zeta converter output with fast ramp sequence

The Output power gains of this ANN and P-O based MPPT techniques using these various converters under rapidly changing irradiance conditions were compared. It is clear that the output power obtained using ANN model is higher than P-O based MPPT for all the three converters. Moreover, ANN based MPPT with Zeta converter exhibits higher efficiency than the other two converters

3.3 Case 3: At change in irradiance with slow ramp sequence

The input as depicted in fig.22 is introduced to the system and its equivalent power output observed employing P-O and ANN based MPPT for three converters are shown in figs.23, 24& 25 respectively.

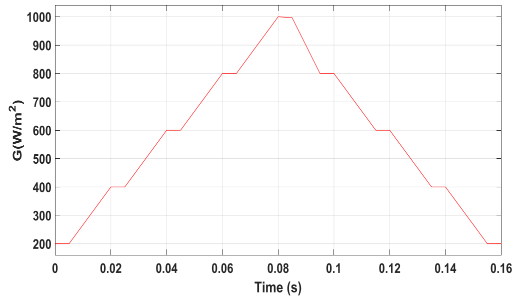

Figure 22: Irradiation change (Slow ramp sequence)

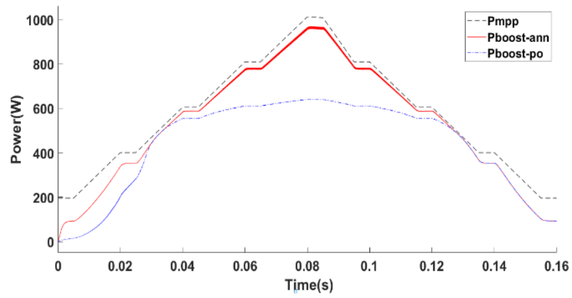

Figure 23: Boost converter output with slow ramp sequence

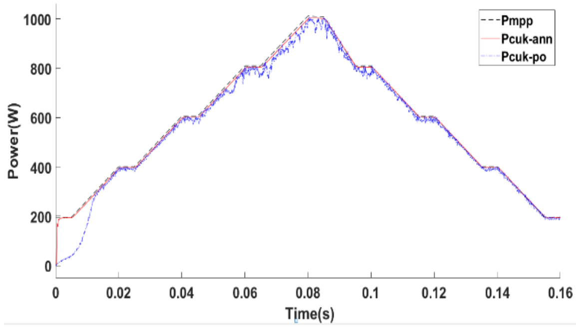

Figure 24: Cuk converter output with slow ramp sequence

 DOI: 10.9790/9622-1204010920

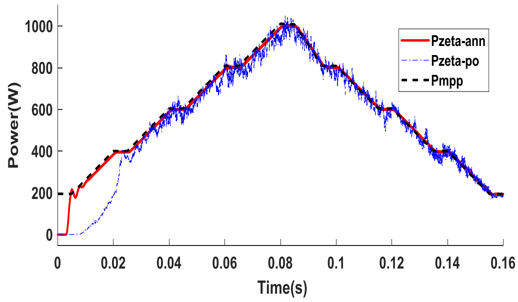

Figure 25: Zeta converter output with slow ramp sequence

It is observed from the figures above P-O based MPPT cannot track MPP under varying atmospheric circumstances. [14] Suggests enhanced P-O with checking algorithm. Although this technique is simple and low-cost, they have several drawbacks. They cannot, for example, achieve high speed and efficiency simultaneously. Furthermore, researchers have lately recognized the sliding mode control (SMC) method for its various strengths, like consistency, parameter variance robustness, dynamic performance, and ease of implementation [15]. However, when applied to a DC/DC converter, this strategy has some drawbacks, like chattering phenomenon. FL technique have the benefit of being centered on PV systems and different knowledge representation. However, they have the disadvantage of being strongly subjective in establishing rules and membership functions. Some drawbacks include the failure to respond quickly during times of varying solar irradiance (G). With low G, the MPPT's precision reduced [16].

On the other hand, the proposed ANN based MPPT provides better tracking and efficient power output for all atmospheric conditions.

Under low irradiance conditions, buck converters perform well for MPPT. The opposite property is possessed by a boost converter. Buck-boost, on the other hand, works well in all irradiance conditions. The main disadvantage is that it has a long response time due to the higher duty cycle changes [17].

It is evident from the results that the boost converter struggles in tracking MPP in low irradiance levels since the point is in the non-operating area. The Cuk converter provides satisfactory performance. Similarly, the Zeta converter also yields a better efficiency and performance rate in all the conditions of irradiances for both slow ramp sequence and fast ramp sequences. The Zeta converters with ANN based MPPT technique provide higher power gains in all atmospheric conditions as well.

3.4 Performance of MPPT controller and Converter

The efficiency of the MPPT controller

$$\eta_{MPPT}=\frac{P_{pv}}{P_{mpp}} \quad (19)$$

Where P_{PV}=PV array's power output and P_{mpp}=Maximum power that can be obtained from SPV array.

The efficiency of the converter

$$\eta_{dc}=\frac{P_{dc}}{P_{pv}} \quad (20)$$

Where Pdc= DC-DC converter's power output.

Table 3 represents the execution of converters at G=1000 w/m^2 and T=25°c.

Table 3 Execution of converters

DC-DC	MPPT	RISE TIME (MS)	SETTLING TIME (MS)	OVER SHOOT (%)	UNDER SHOOT (%)
Boost	P&O	9.46	14.84	2.20	4.20
	ANN	0.87	1.50	0.47	3.15
Cuk	P&O	4.84	-	3.21	5.96
	ANN	0.48	0.83	0.16	2.05
Zeta	P&O	7.62	15.9	4.15	6.12
	ANN	2.1	2.36	0.18	1.98

The overall overshoot-variations and undershoot data variations and the rising time and settling time have been analysed for ANN and P-O methods based MPPT using these three converters. By these data comparisons, it has been depicted that Zeta converters with ANN exhibit a lesser percentage of overshoot and undershoot rate. Cuk converter with ANN exhibits better rise time and settling time. Table 4 illustrates the efficiency comparisons of the converters based on MPPT algorithms using the ANN model and P-O models with uniform conditions.

Table 4 Uniform Condition

CONVERTER	MPPT	η_{MPPT} (%)	η_{DC} (%)
Boost	P-O	95.92	95.34
	ANN	99.60	95.34
Cuk	P-O	96.99	99.19
	ANN	99.6	99.19
Zeta	P-O	97.8	96.2
	ANN	99.7	99.3

From table 4 it is depicted that the converter efficiency of Zeta converter employing Ann model based MPPT is higher than Boost and Cuk converter in uniform conditions. The Zeta converter with ANN provides effective performance under uniform conditions with controller efficiency of 99.7% and converter efficiency of 99.3%. Table 5 demonstrates the efficiency comparisons of the converters based on MPPT algorithms using the ANN model and P&O models with fast ramp sequence. The efficiency of these three converters with P-O and ANN models are estimated.

Table 5 Fast Ramp Sequence

CONVERTER	MPPT	η_{MPPT} (%)	η_{DC} (%)
Boost	P-O	95.6	96.44
	ANN	98.25	96.44
Cuk	P-O	97.59	98.97
	ANN	99.67	99.47
Zeta	P-O	96.5	98.8
	ANN	99.5	99.8

Table 6 Slow Ramp Sequence

CONVERTER	MPPT	η_{MPPT} (%)	η_{DC} (%)
Boost	P-O	90.17	96.44
	ANN	96.79	96.61
Cuk	P-O	97.63	99.0
	ANN	99.69	99.51
Zeta	P-O	96.2	98.6
	ANN	99.5	99.2

From table 5 it is depicted that Cuk and Zeta converter with ANN model provides good performance under a fast ramp sequence. The Zeta converter with ANN provides effective performance with converter efficiency of 99.8%.Table 6 represents the efficiency comparisons of the converters based on MPPT algorithms using the ANN model and P-O models with slow ramp sequence.

The efficiency of these three converters with P-O and ANN modesl are estimated. From table 3 it is depicted that both Cuk and Zeta converter with ANN model provides good performance compared with Boost converter. From tables 4, 5& 6, it is apparent that the presented ANN based MPPT furnishes precise tracking in constant and fluctuating atmospheric circumstances compared with P-O in all the converters.

[18] demonstrates an adaptive incremental resistance procedure that alters the operating point to the Right hand side of the I–V curve in response to adverse changes in irradiance and load resistance. Despite the algorithm's promise of fast tracking, it can steer away from the MPP tracking curve in the presence of dynamically changing irradiance. A voltage reference-based drift-free P&O algorithm that tracks the MPP in the presence of fast - changing irradiance is demonstrated in [19]. The technique, however, has a poor transient stability when exposed to a sudden change in irradiance. To detect a change in irradiance, the methodology in [20] measures up the deviation in power between two samples as well as the voltage of the last two samples. The method, on the other hand, has a slow tracking speed.

But the above results enumerate that the proposed ANN with Zeta converter furnishes efficient performance for varying atmospheric circumstances in all three cases.

IV. CONCLUSION

In this paper, Boost, Cuk and Zeta converter using Neural Network based Maximum Power Point Tracking is designed and analyzed for fluctuating climatic circumstances. The system is designed in a MATLAB/Simulink software for changing atmospheric circumstances. The results demonstrate that the MPPT based on ANN delivers excellent performance when compared with P-O regarding tracking and efficiency under rapidly changing climatic conditions. ANN with Boost converter has poor performance in low irradiance levels and improved execution in high irradiance levels. ANN with Cuk converter delivers satisfactory behavior in all atmospheric circumstances.

Nevertheless, ANN based MPPT controller with Zeta converter exhibited more efficient performance than Cuk converter in all fluctuating climatic conditions with controller efficiency rate of 99.5% and converter's efficiency rate of 99.80% in gaining out maximum power tracking process.

REFERENCES

[1]. J. Prasanth Ram, T. Sudhakar Babu and N. Rajasekar, "A comprehensive review on solar PV maximum power point tracking techniques," *Renewable and Sustainable Energy Reviews*, *vol.67*, pp.826–847, January 2017. doi:10.1016/j.rser.2016.09.076

[2]. Deepak Verma, Savita Nema, A.M.Shandilya, and Soubhagya K.Dash, "Maximum power point tracking (MPPT) techniques: Recapitulation in solar photovoltaic systems," *Renewable and Sustainable Energy Reviews*, *vol.54*, pp.1018–1034, February 2016. doi:10.1016/j.rser.2015.10.068

[3]. Jae-Sub Ko , Jun-Ho Huh ,and Jong-Chan Kim, "Overview of Maximum Power Point Tracking Methods for PV System in Micro Grid", *Electronics* , *Vol* 9, pp. 1-22, 2020. doi:10.3390/electronics9050816

[4]. M.A. Danandeh, S.M. Mousavi G., "Comparative and comprehensive review of maximum power point tracking methods for PV cells", *Renewable and Sustainable Energy Reviews*, *Vol 82*, pp. 2743-2767, 2018. doi:10.1016/j.rser.2017.10.009

[5]. Kah Yung Yap, Charles R. Sarimuthu, and Joanne Mun-Yee Lim, "Artificial Intelligence Based MPPT Techniques for Solar Power System: A review", *Journal of Modern Power Systems and Clean Energy*, *Vol 8*, pp. 1043-1059, 2020. doi:10.35833/MPCE.2020.000159

[6]. Lopez-Guede, J.M., Ramos-Hernanz, J., Altın, N. , " Neural Modeling of Fuzzy Controllers for Maximum Power Point Tracking in Photovoltaic Energy Systems.", *Journal of Electronic Materials* , *Vol 47*, pp. 4519–4532 ,2018. doi:10.1007/s11664-018-6407-2

[7]. R. Reshma Gopi, S. Sreejith, "Converter topologies in photovoltaic applications – A review",*Renewable and Sustainable Energy Reviews*, *Vol.94*, pp.1-14 , 2018. doi:10.1016/j.rser.2018.05.047

[8]. Ehssein, Ba, A., Mahmoud, C.O., M.E.M.O.M. *et al* ,"Comparative Study of Different DC/DC Power Converter for Optimal PV System Using MPPT (P&O) Method",*Appl. Sol. Energy*, *Vol 54*, pp.235-245,2018. doi:10.3103/S0003701X18040047

[9]. Singh, S.P., Gautam, A.K., Tripathi, S.P., Kumar, B , "Performance comparison of MPPT techniques using Cuk converter for photovoltaic energy conversion system" *2017 3rd International Conference on Computational Intelligence & Communication Technology (CICT*), pp 1-6, 2017. doi:10.1109/CIACT.2017.7977369

[10]. Kari Lappalainen and Seppo Valkealahti, "Effects of irradiance transition characteristics on the mismatch losses of different electrical PV array configurations," *IET Renewable Power Generation*, *Vol. 11*, pp. 248-254,2017. doi:10.1049/iet-rpg.2016.0590

[11]. Erickson, R.W , " DC–DC Power Converters", *In Wiley Encyclopedia of Electrical and Electronics Engineering*, J.G. Webster (Ed.), 2007. doi:10.1002/047134608X.W5808.pub2

[12]. Sarvi, M., Azadian, A., "A comprehensive review and classified comparison of MPPT algorithms in PV systems", *Energy System*, 2021. doi:10.1007/s12667-021-00427-x

[13]. R. Divyasharon, R. Narmatha Banu and D. Devaraj, "Artificial Neural Network based MPPT with CUK Converter Topology for PV Systems Under Varying Climatic Conditions," *2019 IEEE International Conference on Intelligent Techniques in Control, Optimization and Signal Processing (INCOS*), 2019, pp. 1-6, doi: 10.1109/INCOS45849.2019.8951321

[14]. Alik, R. and A. Jusoh, " An enhanced P&O checking algorithm MPPT for high tracking efficiency of partially shaded PV module", *Solar Energy*. *Vol. 163*, pp. 570–580, 2018. doi: 10.1016/j.solener.2017.12.050.

[15]. P. A. O. Valencia and C. A. Ramos-Paja, "Sliding-mode controller for maximum power point tracking in grid-connected photovoltaic systems", *Energies*, *Vol 8*, pp. 12363– 12387, 2015. doi:10.3390/en81112318

[16]. Shiau, J.K.; Wei, Y.C.; Chen, B.C, "A Study on the Fuzzy-Logic-Based Solar Power MPPT Algorithms Using Different Fuzzy Input Variables", *Algorithms*, 2015, *Vol 8*, pp.100–127, 2015. doi:10.3390/a8020100

[17]. Mustafa Engin Başoğlu, Bekir Çakır, "Comparisons of MPPT performances of isolated and non-isolated DC–DC converters by using a new approach",*Renewable and Sustainable Energy Reviews*, *Vol 60*, pp. 1100-1113, 2016. doi:10.1016/j.rser.2016.01.128

[18]. M. Gunasekaran, V. Krishnasamy, S. Selvam, D. J. Almakhles and N. Anglani, "An Adaptive Resistance Perturbation Based MPPT Algorithm for Photovoltaic Applications," IEEE *Access*, *vol. 8*, pp. 196890-196901, 2020, doi: 10.1109/ACCESS.2020.3034283.

[19]. M. Killi and S. Samanta, "Voltage-Sensor-Based MPPT for Stand-Alone PV Systems Through Voltage Reference Control," *IEEE Journal of Emerging and Selected Topics in Power Electronics*, *vol. 7*, no. 2, pp. 1399-1407, June 2019, doi: 10.1109/JESTPE.2018.2864096.

[20]. H. Abouadane, A. Fakkar, D. Sera, A. Lashab, S. Spataru and T. Kerekes, "Multiple-Power-Sample Based P&O MPPT for Fast-Changing Irradiance Conditions for a Simple Implementation,"*IEEE Journal of Photovoltaics*, *vol. 10*, no. 5, pp. 1481-1488, Sept. 2020, doi: 10.1109/JPHOTOV.2020.3009781.

R Divyasharon, et. al. "Performance assessment of Boost, Cuk and Zeta converter with Neural Network MPPT in PV Systems for Varying Weather Patterns." *International Journal of Engineering Research and Applications (IJERA)*, vol.12 (04), 2022, pp 09-20.